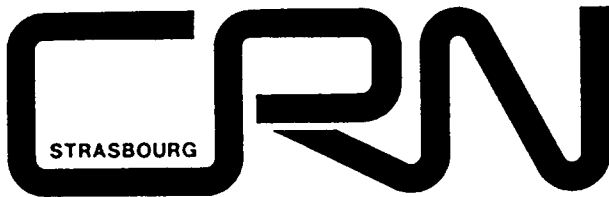


BB



CRN 95-35

**GAMOW-TELLER AND COMPETING FORBIDDEN
TRANSITIONS FAR FROM STABILITY**

G. WALTER

Centre de Recherches Nucléaires et Université Louis Pasteur
67037 Strasbourg Cedex 2 (France)

*Contribution to ENAM 95
"International Conference on Exotic Nuclei and Atomic Masses"
ARLES (France) June 19-23, 1995*



CERN LIBRARIES, GENEVA

SW 9543

**CENTRE DE RECHERCHES NUCLEAIRES
STRASBOURG**

IN2P3
CNRS

UNIVERSITE
LOUIS PASTEUR

GAMOW-TELLER AND COMPETING FORBIDDEN TRANSITIONS FAR FROM STABILITY

G. WALTER

Centre de Recherches Nucléaires
B.P.28 - 67037 Strasbourg Cedex2 (France)

Abstract

Some general properties of nuclei far from stability which are determined by Gamow-Teller matrix elements are discussed and compared to theoretical predictions. The discussion is limited to light proton-rich nuclei for which a more precise determination of the GT strength is obtained. The deviation observed in the interpretation of some sd nuclei with shell model calculations are illustrated by the case of the ^{38}Ca decay. Interrelations between values obtained in decay or charge-exchange reactions studies are outlined in the case of fp nuclei for which new theoretical results allow to extend the description given by partial experimental data. Finally, the possible observation of 1st forbidden transitions far from stability is illustrated with a few examples.

Introduction

The Gamow-Teller spin-isospin excitation and the measurement of its strength give access to important matrix elements. These m.e. provide a sensitive test of the multiparticle structure of nuclear wave functions and also of the different correlations which reduce the observable strength. Among the possible probes of spin excitation (by weak, electromagnetic or strong interaction), we limit here the discussion to complementary results obtained either in the weak decay study of p-rich nuclei or with charge exchange processes such as (p,n) reactions. With the hadronic probe, it is possible to map out the full range of spin-isospin excitation at small or high momentum transfer. It is therefore the best tool to investigate the spin-isospin mode and search for possible missing strength by comparison with theoretical estimates.

In the nuclear β^+ decay, the Gamow-Teller transition results from the coupling of the axial-vector current with the spin of the nucleon. Within the accessible Q_β energy window accurate measurements of the GT strength can be made with excellent resolution, high sensitivity and low background. For p-rich nuclei, and also for nuclei near closed shells, the strongest transitions (i.e. the major part of the strength) may be included in the Q_β window. For these selected cases, excellent conditions are met for a state-by-state, or an overall, comparison of the corresponding matrix elements with theoretical predictions and a quantitative evaluation of the reduction (quenching) of the experimental strength. These two excitation modes are sketched in Fig. 1, their interrelations with

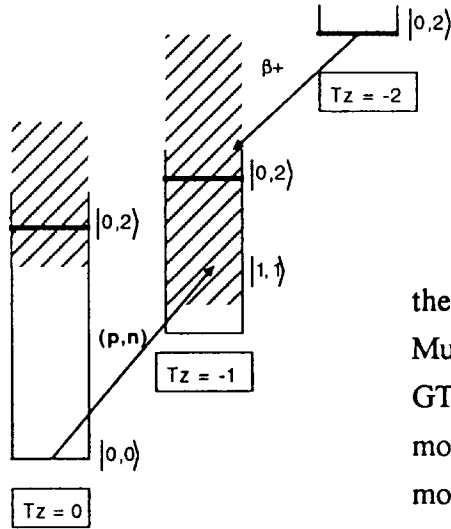


Fig.1 : GT transitions in the case of a light $A=4n$ system, stemming from states with different isospin and populating levels in the same final nucleus.

the electromagnetic modes (e , e' or γ , γ') have been discussed by W. Muller et al.¹⁾. From extensive comparisons between experimental GT decay rates and theoretical values calculated in p , sd or fp shell model configuration an excellent agreement has been observed, in most of the cases, with an overall reduction of $m.e.$ by a factor 0.76. The resulting predictive power of these calculations is of interest in

two different fields :

- the description of nuclear properties far from stability
- the estimation of weak interaction rate in stellar evolution. In the current studies undertaken to calculate weak interaction rates in stellar matter, the electron capture rate plays a major role at advanced stage of stellar evolution²⁾. The capture rate for a transition from the i -th state of the (Z,N) nucleus to the j -th state in the $(Z+1, N-1)$ nucleus, is given by ³⁾ :

$$\lambda_{ij} = \frac{\ln 2}{D} B_{ij} g_{ij} \quad (1)$$

where D is expressed by universal constants,

$$B_{ij} = B(F)_{ij} + (g_A / g_V)^2 B(GT)_{ij} \quad (2)$$

corresponds to the reduced Fermi and GT transitions and g_{ij} is the phase space integral. The same quantities are necessary to calculate the neutrino energy loss rate and the γ heating rate. These calculations are extremely sensitive to the details of nuclear structure through phase-space considerations and therefore the experiments providing GT rates in the large energy range open in the decay of p -rich nuclei are very profitable tests of the shell-model calculations.

GT transitions in proton-rich sd nuclei. Shell-model estimates / experimental results

For these decays, a first comparison between predicted and measured GT strength can be made with half-life values. This property, apart from a contribution of the Fermi component, reflects the distribution of the main GT transitions. It is often the only available information near the drip-line. $T_{1/2}$ values, calculated by Muto et al.⁴⁾ in a complete sd -space shell model with the effective Hamiltonian of Wildenthal⁵⁾, are compared for $T_z = -3/2$ with experimental values in Fig.2. The excellent agreement is a convincing argument for using far from stability the quenching factor for the

GT transitions operator previously established with existing data in the sd-shell⁶⁾:
 $[\gamma^2 = (g_A^{eff} / g_A)^2 = (0.76)^2]$.

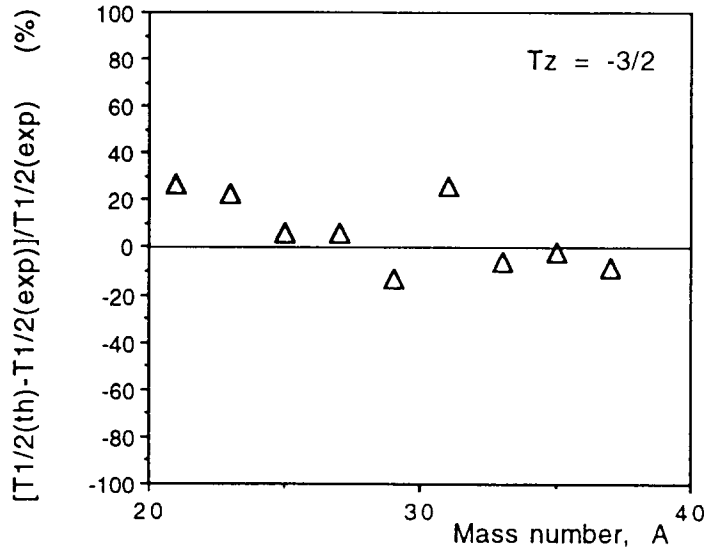
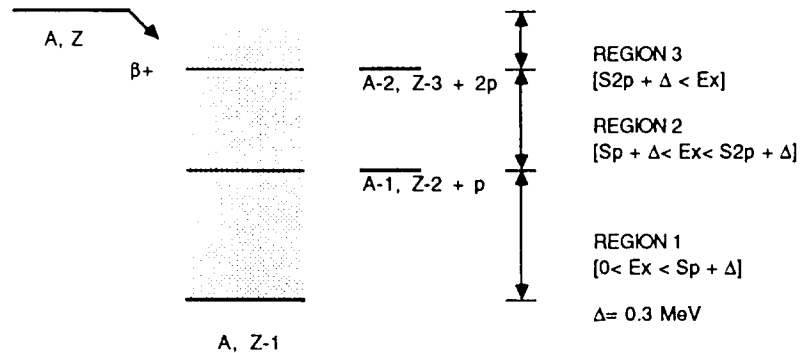


Fig.2 : Relative difference between experimental values (from the literature) and shell model evaluations (Muto et al.⁴⁾) for proton rich $T_z = -3/2$ sd shell nuclei.

In order to compare more precisely experimental data with GT estimates, it is useful to discern⁴⁾ different regions in the final nucleus excitation range corresponding to different decay channels following upon the GT transition (Fig.3). It is also important to note that the sensitivity of the experiment/calculation comparison is different in these three regions. We have plotted in Fig.4 the summed branching strength (expressed as a β percentage of the total decay) corresponding to the different region defined in Fig.3 and resulting from sd-shell calculations by Muto et al.⁴⁾.

Fig.3 : Different ranges of E_x populated by GT transitions in p-rich nuclei. Detailed GT analysis is often limited to region 1 and 2. The energy step, Δ , is introduced to take the proton penetrability into account⁴⁾.



For 6 cases [^{21}Mg , ^{29}S , ^{33}Ar , ^{37}Ca ($T_z = -3/2$) and ^{36}Ar , ^{36}Ca ($T_z = -2$)] where detailed results have been reported, experimental value of P_p (1-delayed proton emission probability) are found in fair agreement while more precise experimental results are needed for an extended comparison. With present data, calculated strength in region 2 ($T_z = -2$) exceeds by far measured values of P_p in many cases where more work would certainly be justified. Many interesting features are however already apparent in the A and T_z evolution of the calculated intensities.

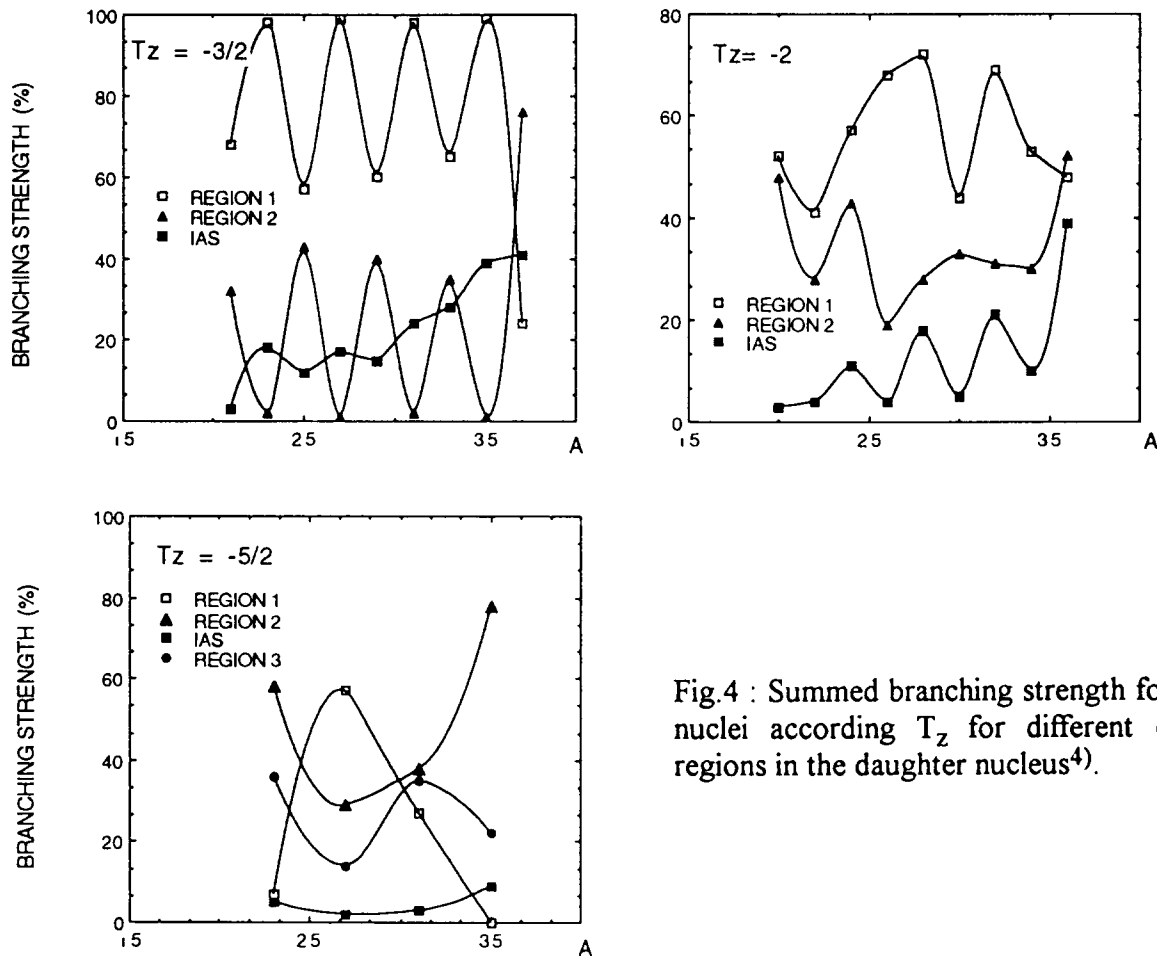


Fig.4 : Summed branching strength for sd-shell nuclei according T_z for different excitation regions in the daughter nucleus⁴⁾.

If we compare experimental and predicted sums of $B(GT)$ values for nuclei where this comparison can be done, we obtain a diagram (Fig.5) similar to the one given previously by Borge et al.⁷⁾ where most results are well described with a renormalized coupling constant and some cases are clearly anomalous. Especially for the argon isotopes, the quenching factor seems to be greatly reduced or even nonexistent (^{33}Ar). However the comparison, made in Fig.5, is model dependent with different degrees depending the individual decay. In particular :

- the fraction of total GT strength which is measured is different from isotope to isotope,
- in some cases, as for the $T_z = -3/2$ nuclei, the experimental cut-off is close to the maximum of the GT resonance, the ratio of experimental to calculated strength is then drastically model dependent with a very large uncertainty on the resulting value. Until recently this absence of quenching seemed to be specific to the argon isotopes but new investigations of the ^{37}Ca decay⁸⁾ have suggested in the same way that a renormalization of the axial-vector current is not supported by the comparison of the data with sd shell model calculations. More accurate data on p-rich Ca nuclei were required.

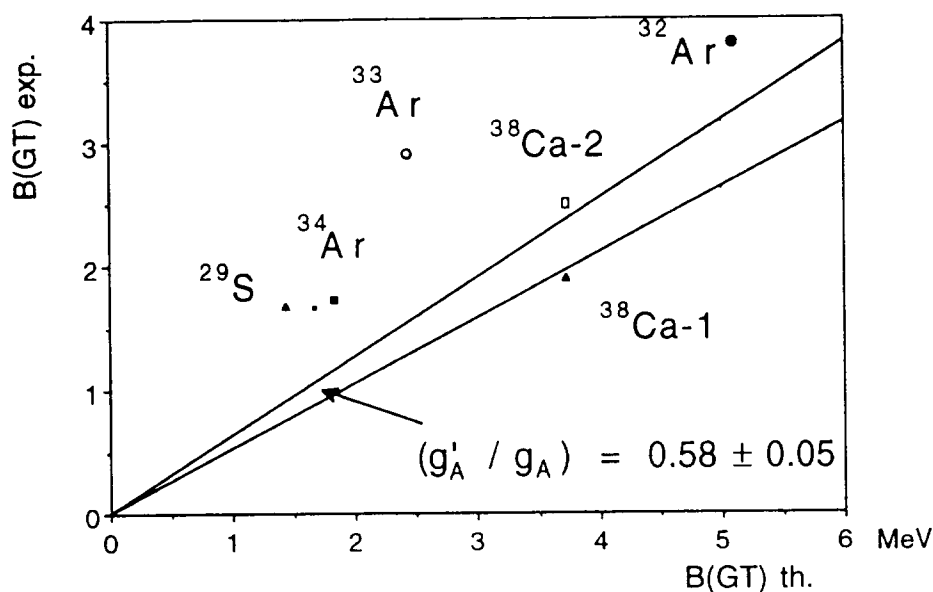
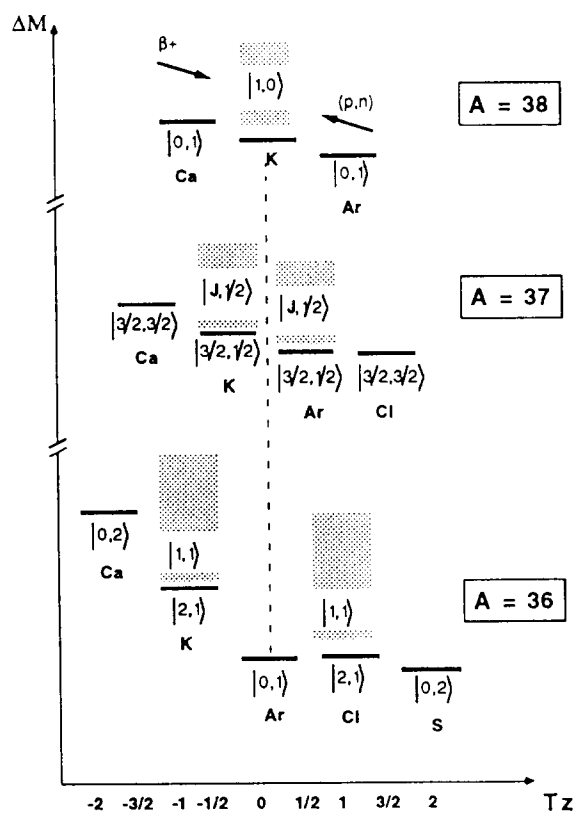


Fig.5 : Observed and calculated GT strengths for some β^+ decays which deviate from the bulk of sd-shell results, located between the two solid lines⁷⁾. Results are expressed in $\langle\sigma\tau\rangle^2$ units. Two values are indicated for ^{38}Ca , corresponding to Ref.6 (low exp. value) and Ref.12 (high exp. value).

The case of the Ca isotopes : $^{38}\text{Ca}(\beta^+)^{38}\text{K}$ decay

In Fig.6 are represented the mass diagram corresponding to three isobaric multiplets where β^+ decays of the Ca member have been studied and results reported at this conference⁹⁻¹¹⁾. In two cases ($A = 37$ and 38) matrix elements resulting from (p,n) studies are available and can be compared to beta decay values. The ^{38}Ca case, with a modest Q_β value, is of particular interest for different reasons :



- direct population of ^{38}K by β^+ or (p,n)
- very simple 2 holes structure of the ^{38}Ca parent state
- excellent experimental condition available for both production and detection
- and, most important, for ^{38}Ca a very large fraction of the GT strength lies within the β decay Q value window.

Fig.6 : Mass diagram for $A=36-38$ with β^+ and (p,n) GT excitation modes.

This property is manifest when evaluating the theoretical value of the sum $T(GT)$, defined by ⁶⁾ :

$$T(GT) = \left[\sum_f R^2(GT, i \rightarrow b) \right]^{1/2} \quad (3)$$

where $R(GT) = M(GT)/W$ (4)

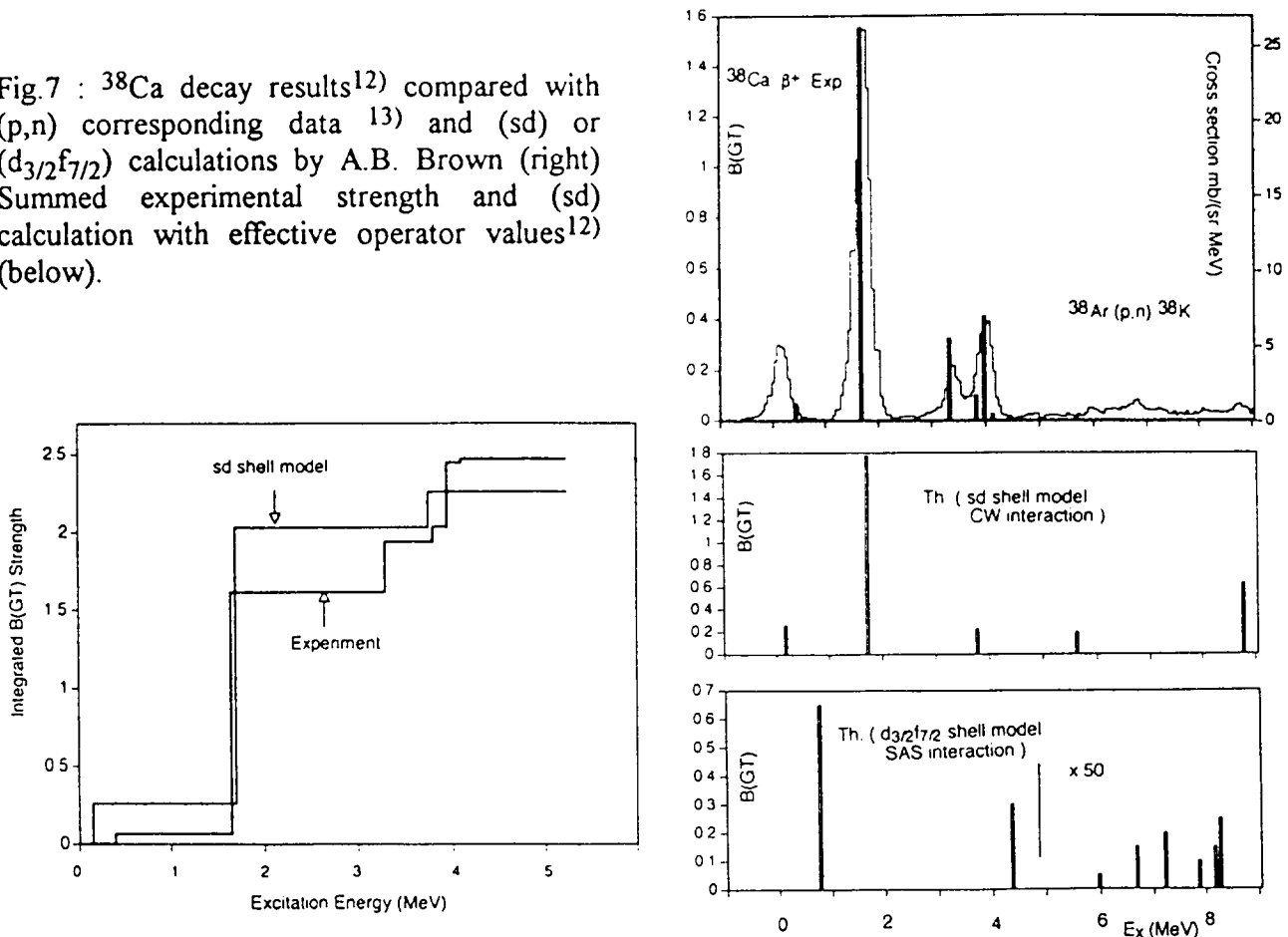
is a dimensionless quantity obtained after introducing the sum rule value :

$$W = |g_A / g_V| \left[(2J_i + 1) 3 | (N_i - Z_i) | \right]^{1/2} \quad (5)$$

Using theoretical values calculated with the "free-nucleon" Gamow-Teller operator⁶⁾, $T(GT) = 0.78$ for ^{38}Ca and only 0.38 for ^{37}Ca . The strength in ^{38}K is concentrated in the lowest-lying 1^+ states and is shifted to higher excitation energies as the proton excess is increased in $^{37,36}\text{K}$, in close analogy with the evolution of β^- strength with increasing neutron excess, near closed shells.

In the ^{38}Ca decay study by Baumann et al.¹²⁾, production yields of pure Ca sources by fluorination in the ISOLDE ion source and efficient β - γ measurements allowed a sensitivity around 40 p.p.m. for the population of the 1^+ states. $B(GT)$ determination, reported in Fig.6, are compared to (p,n) zero degree cross section measurements obtained by Anderson¹³⁾ and populating the same final nucleus. Shell model predictions by A.B. Brown with two different configuration spaces, are also reported. Two important points can be highlighted (Fig.7) here :

Fig.7 : ^{38}Ca decay results¹²⁾ compared with (p,n) corresponding data ¹³⁾ and (sd) or ($d_{3/2}f_{7/2}$) calculations by A.B. Brown (right) Summed experimental strength and (sd) calculation with effective operator values¹²⁾ (below).



- The (p,n) measurement confirms that 80 % of the strength is located within the Q_β window where the high resolution β -delayed gamma measurement can resolve branches to six 1^+ final states.
- From these six 1^+ states, three can be interpreted with the sd-shell model while the $d_{3/2} f_{7/2}$ calculation allows to locate intruder 1^+ states as low as 4 MeV in agreement with the experimental findings.

The new experimental summed strength is reported in Fig.5. In fact the additionnal strength being due to intruder states, this representation is no longer valid and another normalization is needed to take into account the increase of model space. The total S^+ strength :

$$S^+ = 3(Z - N) + S^- \quad (6)$$

strictly limited to $3(Z-N) = 6$ in the sd space, is increased when the f contribution allows S^- to have a sizeable value. The evaluation of S^- in this case is still to be made. It is of interest to note that for a similar 2 holes-case, Hardy and Towner¹⁴⁾ have reported an increase from 6 to 7.1 of the S^+ value when adding 2p4h configurations to the p-shell description of ^{14}O .

The same restriction has to be made with the integrated strength representation of Fig.7 (lower left). The apparent excess of experimental strength, relative to the calculation with effective operator values, may be only a deluding result related to the sd-space limitation when the experimental data clearly require an extended configuration.

What are the changes we can expect in the GT strength of Ca isotopes when going from ^{38}Ca to ^{36}Ca ? Intruder states are still located in the same energy ranges as it is shown by the comparison of experimental levels with sd calculations. On the other hand the increase of Q_{EC} (from 6.74 MeV for $A=38$ to 10.99 MeV for $A=36$) and phase space arguments give a strong enhancement in the population of these intruder states. In addition, the increase of ground state correlations resulting from the increment of valence nucleons should induce a shift of the GT strength to higher energy.

In conclusion, the proton-rich nuclei in the sd-shell present at low energy alien configurations which are populated with increasing probability by GT transitions when going away from stability. This nuclear structure effect is revealed as deviation from sd shell model expectations and can be traced already in simple cases like the ^{38}Ca decay.

GT transitions in fp shell nuclei. $T_z = -2$ drip-line nuclei and $T_z = +2$ charge-exchange target nuclei

Recent theoretical studies give a microscopic description and a successful account of many observable for stable or unstable fp nuclei. In particular detailed shell model calculations of the GT strength for $A = 48$ ¹⁵⁾, 54 and 56¹⁶⁻¹⁷⁾ have been made and a good agreement has been found with the available (p,n) data. Very recently, Nowacki et al.¹⁸⁾ have extended these calculations to the description of the beta decay of the $T_z = -2$ drip-line nuclei between ^{44}Cr and ^{56}Zn . Allowed transitions from ^{44}Cr , ^{46}Mn , ^{48}Fe , ^{50}Co , ^{52}Ni and ^{56}Zn have been evaluated (^{54}Cu is predicted

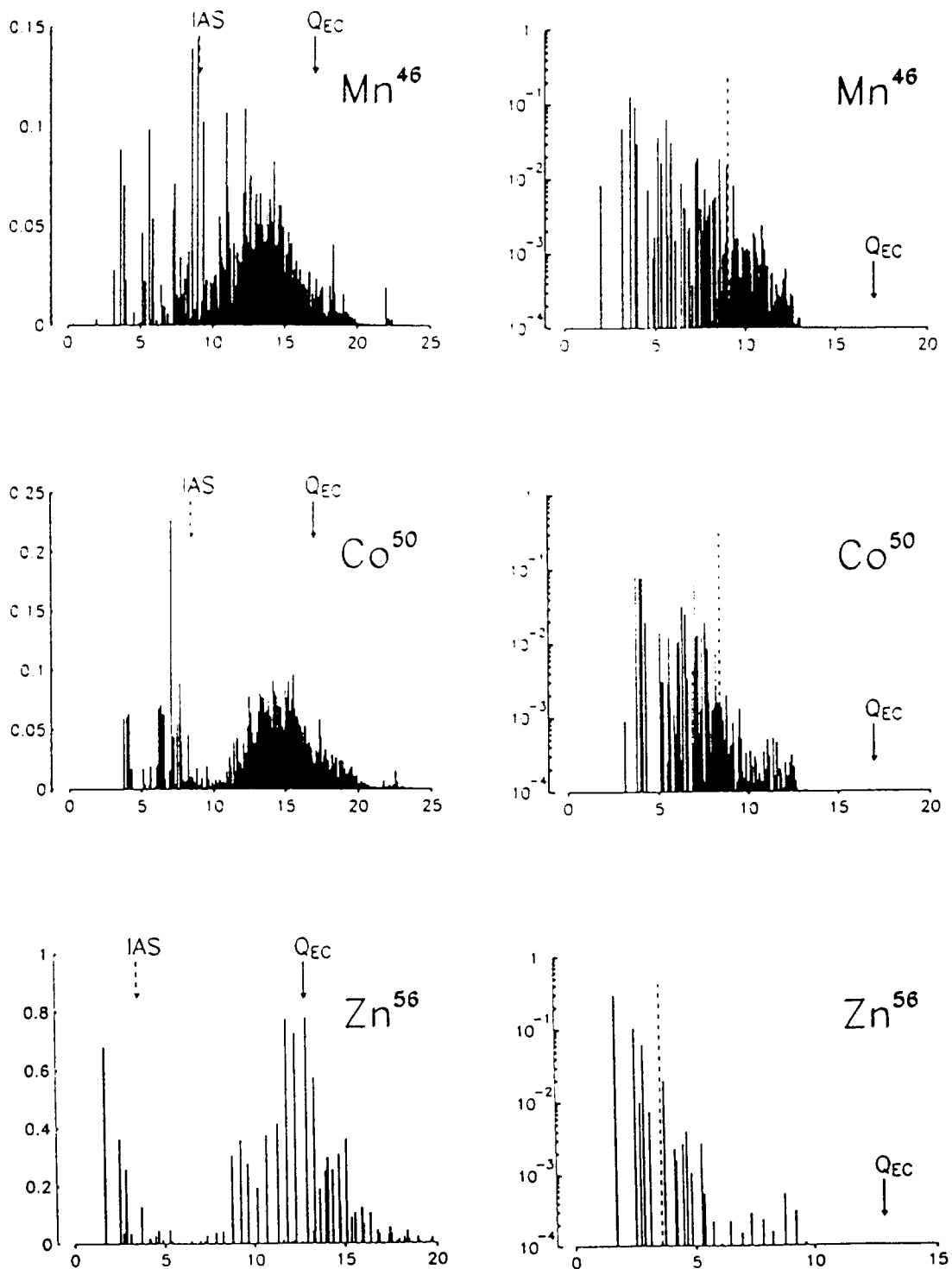


Fig.8 : From Nowacki et al.¹⁸⁾. Left part : B(GT) values for three $T_z = -2$, fp nuclei. Right part : same results expressed as beta branching strength. The vertical log scale has been arbitrarily limited to 10^{-4} . Note the dilatation of the horizontal scale.

unbound). For the even-even parent nuclei, daughter 1^+ states in ^{44}V , ^{48}Mn , ^{52}Co and ^{56}Cu are members of the isobaric triplets which have been already studied in ^{44}Sc , ^{48}V , ^{52}Mn and ^{56}Co . The odd-odd ^{46}Mn and ^{50}Co parent states are expected to have, respectively $J^\pi = 4^+$ and 6^+ on their analogues in the isobaric quintuplets (^{46}Sc and ^{50}V). Results obtained by F. Nowacki¹⁸⁾ for three $T_z = -2$ nuclei are reported in Fig.8 in two different ways. On the left side, the B(GT) distribution reveals the density of transitions, increasing with the number of valence nucleons and, for ^{48}Fe and ^{52}Ni , the resonant-like structure with a maximum below the Q_{EC} limit. On the right side, converting B(GT) values in β branches intensities, one brings to light the difficulty for giving an experimental description of the strength in the whole window. Recent advances have been made in the spectroscopy of $T_z = -2$ nuclei¹⁹⁻²²⁾ but detailed comparison of branching GT strength with calculation is still difficult. On the other hand, except for ^{56}Zn , half-lives have been measured¹⁹⁻²²⁾ and are found in excellent agreement with the shell model estimates, in particular for the even-even nuclei ($\Delta T_{1/2} \leq 10\%$).

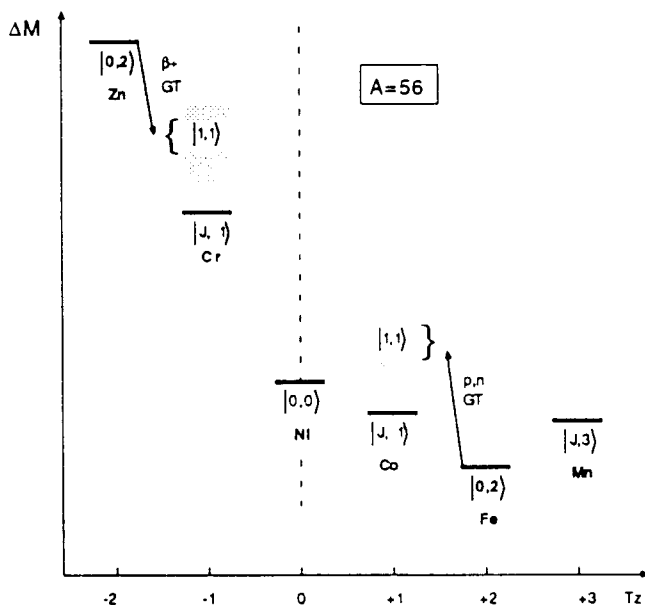


Fig.9 : Multiplet of $A = 56$ isobars.

The mass diagram corresponding to the fp isobars with $A = 56$ is given in Fig.9 in order to illustrate the possible GT studies in this mass region. Unlike sd-nuclei, the stable member of the multiplet has $T_z = +2$ (^{56}Fe) while the analog $T_z = -2$, ^{56}Zn is the last bound isobar.

Many properties of this drip-line nucleus can therefore be deduced from its stable counterpart. In particular GT decay properties are given by matrix elements which can be extracted from 0° charge-exchange cross-sections measured on the analogue isobar.

Extracting GT matrix elements from (p,n) cross-sections ; application to decay properties estimations near the drip-line

The accuracy of the determination of GT matrix elements and the correlation between beta decay and (p,n) determination have been recently discussed by Ch. Goodman²³⁾. As a good correspondence is found for GT values obtained with the two different probes for transitions between $J^\pi = 0^+$ and 1^+ , we can choose the case of the ^{56}Fe (p,n) reaction for the determination of GT matrix elements which govern decay rates at the drip-line. As shown in Fig.9, ^{56}Fe ground state (0^+ , $T_z = 2$) is the analog of the very proton rich ^{56}Zn g.s.. Decay properties of the $T_z = -2$ exotic

emitter are unknown but the (p,n) reaction on the $T_z = +2$ target has been measured by J. Rapaport et al.²⁴⁾ and the corresponding cross-section measurement at 0° is given after background subtraction in Fig.10. In a low momentum transfer approximation, the cross-section is related to $B(GT)$ as follows²³⁾ :

$$d\sigma/d\omega(0^\circ) = (\mu/\pi\hbar^2)^2 (K_f/K_i) N_{\sigma\tau} J_{\sigma\tau}^2 B(GT) \quad (7)$$

if we omit the Fermi, $B(F)$ contribution.

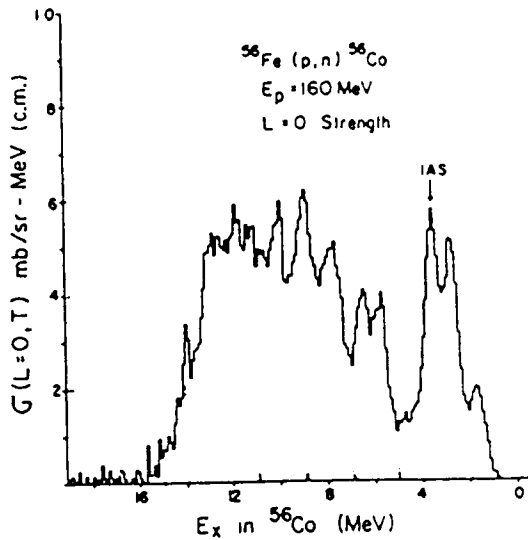


Fig.10 : From J. Rapaport²⁴⁾, cross-section of the $^{56}\text{Fe}(p,n)^{56}\text{Co}$ reaction measured at 0° .

Two parameters, $N_{\sigma\tau}$, the distortion factor, and $J_{\sigma\tau}$, the effective interaction strength are obtained by normalization of the (p,n) to the beta decay probe for transitions where accurate data are obtained in both ways.

Dividing the spectrum of Fig.10 in energy bins, we can then, using relation (7), obtain a $B(GT)$ distribution where :

$$B_i(GT) = \sum_{E_i}^{E_i + \Delta E} B(GT) \quad (8)$$

The $B(GT)$ value is related to the partial half-life in decay rates evaluations by :

$$1/ft = g_V^2 B(F) + g_A^2 B(GT) \quad (9)$$

The $B_i(GT)$ distribution is then converted in a set on partial half-lives, t_i $B_i(GT) \rightarrow f_i t_i$

and
$$(T_{1/2})^{-1} = \sum_i (t_i)^{-1} \quad (10)$$

Using the experimental (p,n) cross-sections of Rapaport²⁴⁾ we obtain for ^{56}Zn : $T_{1/2} = 36 \pm 10$ ms.

This determination can be compared to the theoretical shell-model calculation of Nowacki¹⁸⁾ ($T_{1/2} = 24$ ms).

1st forbidden transition in competition with allowed GT decays far from stability

Beta decay studies with exotic nuclei are often limited to the most intense transitions and therefore to superallowed or allowed branches. However forbidden transition can also be involved in these studies and particularly in two cases :

- a) When the detection sensitivity is very high. This condition is met for delayed charged particle detection. For light nuclei, where forbidden transitions are clustered near magic numbers, it is remarkable that the only forbidden transitions known in the mass range $22 < A < 36$ are in the

^{32}Cl , 1^+ decay and correspond to very weak alpha delayed ($2 \cdot 10^{-6}$) or proton delayed ($19 \cdot 10^{-6}$) branches²⁵).

b) When the transition rates are comparable to allowed ones.

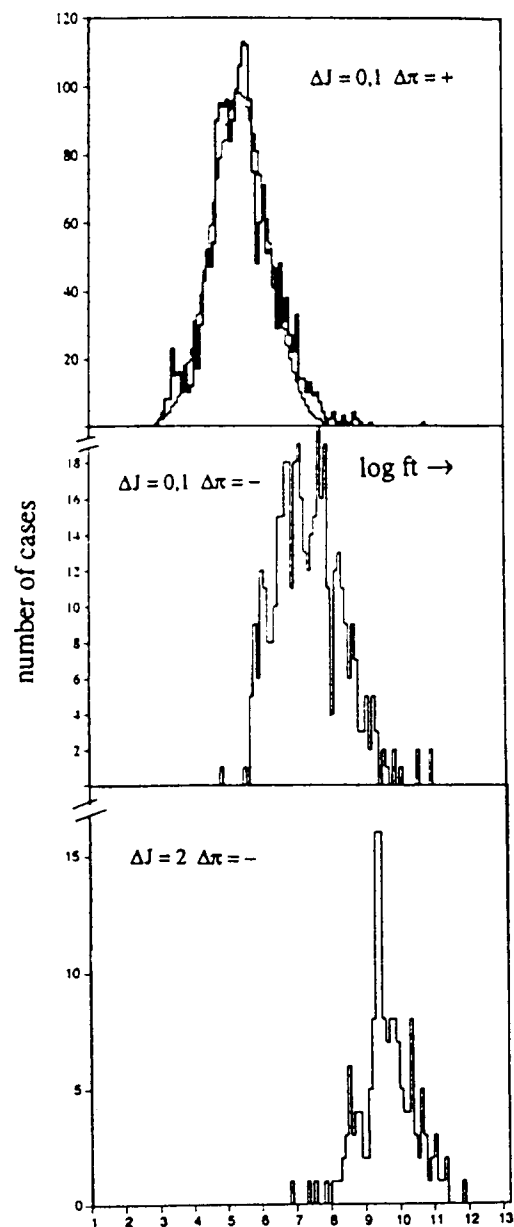
Previous compilations²⁶) of comparative half-lives, expressed with $\log ft$ values, allow to delineate the range of the different classes of beta transitions. Unfortunately these compilations do not include more recent data which are mostly obtained far from stability. A new survey has been made recently²⁷) for $10 < A < 100$ with data corresponding to reliable spins and parity. From the results (Fig.11) a strong overlap between $\log ft$ values for allowed and 1st forbidden non unique transitions is confirmed and more precisely described. These distribution suggest also some modifications of the empirical rules given by Raman and Gove²⁸) for spin and parity limitations from $\log ft$ values.

Fig.11 : Frequency distribution of $\log ft$ values for allowed (2227 cases), 1st forbidden non unique (424 cases) and 1st forbidden unique (157 cases) transitions given in the literature in the $10 < A < 100$ range (Ref.27). In the two first classes, $\log ft$ values are reported ; for the last class, $\log f_1 t$ values are given.

The studies of 1st forbidden β transitions has allowed previously²⁹) to verify the prediction made by Kubodera et al.³⁰) of a strong enhancement over the impulse approximation for the time-like component, M_o^T , of the axial current, A° . This enhancement, due to meson-exchange contributions (mec) is studied most easily with transitions between states of the same spin (as $0^+ \rightarrow 0^-$) and it can be quantified by the ratio, ϵ_{mec} , of the experimental A° value, to the calculated one obtained in the impulse approximation without meson-exchange contribution :

$$\epsilon_{mec} = [A^\circ(1part) + A^\circ(mec)] / A^\circ(1part)$$

with experimental values corresponding to $s_{1/2} \leftrightarrow p_{1/2}$ transitions and A values around 16 or 96, the strong enhancement is confirmed and a mean value of $\epsilon = 1.64(2)$ has been obtained³¹).



The situation is unsatisfactory for $p_{3/2} \leftrightarrow d_{5/2}$ transitions. This class includes cases with enhanced values for ϵ [$^{38}\text{S}(0^+) \rightarrow ^{38}\text{Cl}(0^-)$, $\epsilon_{\text{mec}} = 1.13$, $^{29}\text{K}(0^-) \rightarrow ^{50}\text{Ca}(0^+)$, $\epsilon_{\text{mec}} = 1.52$ ³³⁾] and cases where the 1st forbid transition is much lower than the shell-model estimate in the impulse approximation [$^{38}\text{Ca}(0^+) \rightarrow ^{38}\text{K}(0^-)$ ¹²⁾, $^{39}\text{Ca}(3/2^+) \rightarrow ^{39}\text{K}(3/2^-)$ ³⁵⁾, $^{37}\text{K}(3/2^+) \rightarrow ^{37}\text{Ar}(3/2^-)$ ³⁶⁾]. Clearly more studies are needed before a clear picture of mesonic enhancement effects comes out in the full range of atomic masses and nuclear configurations.

Conclusion and outlook

Efficient production and detection techniques allow in many cases a better determination of the GT distribution in the Q_β window and the measurements of weak branches which give significant tests for the models. These measurements allow also the evaluation of other classes of transitions (isospin forbidden, $J \rightarrow J$ 1st forbidden) which give access to subnuclear processes.

The intercorrelation of beta decay results and charge exchange studies which can be illustrated by different examples in the sd and fp shells may be extended with the use of radioactive ion beams. In the fp shell, present conditions for GT studies are unsatisfactory : detailed microscopic description of p-rich nuclei decay are available but, the comparison with experimental data is limited as efficient ion sources are not yet available for many of these elements.

A more general limitation of the experiment/theory comparison is noted in an extended mass range which includes most of the p-rich sd nuclei. It corresponds to the difficulty to include intruder configurations in the model space when these configurations are clearly borne out by the experimental data. For neutron-rich nuclei, this limitation is evidently still more general.

Finally, next GT studies should include transitions of particular interest : beta branches to states in halo nuclei or beta transitions to unbound levels from proton even (^{69}Kr , ^{39}Ti) or neutron even emitters (^{37}Na) at the very limit of nuclear stability.

REFERENCES

1. W. Müller et al., Nucl. Phys. A430 (1984) 61
2. G.M. Fuller et al., Astrophys. J. Suppl. 42 (1980) 447
3. T. Oda et al., Atomic Data and Nucl. Data Tables 56 (1994) 231
4. K. Muto et al., Phys. Rev. C43 (1991) 1487
5. B.H. Wildenthal, Prog. Part. Nucl. Phys. 11 (1983) 5
6. B.A. Brown and B.H. Wildenthal, Atomic Data and Nuclear Data Tables 33 (1985) 347
7. M.J.G. Borge et al., Z. Phys. A332 (1989) 413
8. E.G. Adelberger et al. Phys. Rev. Lett. 67 (1992) 3658
9. W. Trinder et al., Phys. Lett. B348 (1995) 331
10. W. Trinder et al., Phys. Lett. B349 (1995) 267
11. W. Trinder et al., Contribution to this Conference
12. P. Baumann et al., (1995) to be published
13. B.D. Anderson et al., to be published and private communication

14. J.C. Hardy and I.S. Towner, *J. Physique C4* (1984) 417
15. E. Caurier et al., *Phys. Rev. C50* (1994) 225
16. E. Caurier et al., *Phys. Rev. Lett.* (1995) 1517
17. E. Caurier et al., (1995) to be published
18. F. Nowacki et al., (1995) to be published
19. L. Faux et al., *Phys. Rev. C49* (1994) 2440
20. B. Blanck, Contribution to this Conference
L. Faux, Thesis (Bordeaux, 1995)
21. V. Borrel et al., *Proc. 6th Int. Conf. on Nuclei far from Stability, Bernkastel-Kues* (1992)
22. V. Borrel et al., Internal Report Orsay, IPNO-DRE 92-17
23. Ch. D. Goodman, *Nucl. Phys. A577* (1994) 3c
24. J. Rapaport et al., *Nucl. Phys. A410* (1983) 371
25. J. Honkanen et al., *Nucl. Phys. A330* (1979) 429
26. H. Behrens, *Proc. Int. Conf. Nucl. Physics, Berkeley* (1980) LBL-11118 p.817
27. F. Didierjean and G. Walter, *Strasbourg, CRN Report 94-01*
28. S. Raman and N.B. Gove, *Phys. Rev. C7* (1973) 1995
29. E.K. Warburton et al., *Annals of Physics* 187 (1988) 471
30. K. Kubodera et al., *Phys. Rev. Lett.* 40 (1978) 755
31. E.K. Warburton et al., *Phys. Rev. C49* (1994) 824
32. H. Mach et al., *Phys. Rev. C41* (1990) 226
33. E.K. Warburton, *Phys. Rev. C44* (1991) 1024
34. G. Walter, *Proc. Workshop Nucl. Structure of Light Nuclei far from Stability, Obernai 1989*,
Ed. G. Klotz, Strasbourg, 1990
35. E. Hagberg et al., *Nucl. Phys. A571* (1994) 555
36. E. Hagberg (1995) private communication